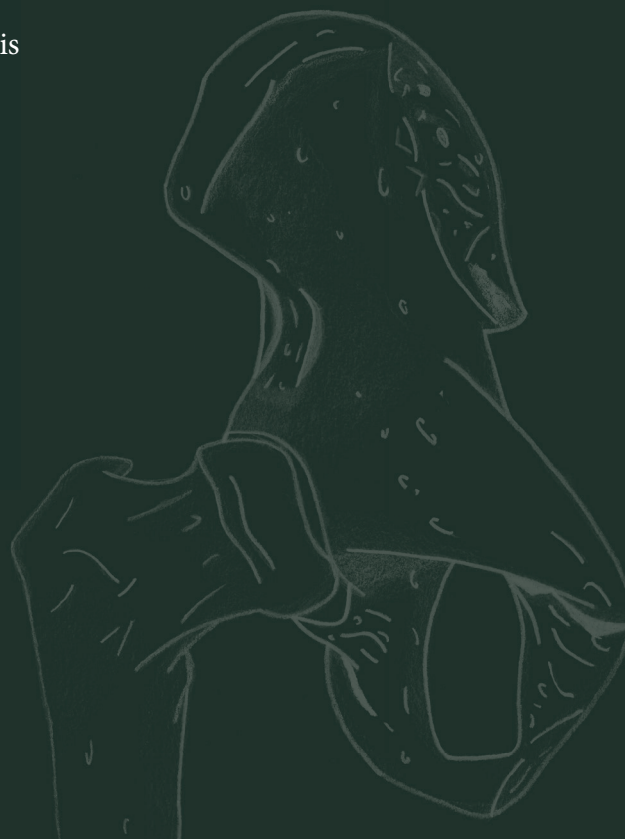


Dynamic model-based Radiostereometric Analysis for Evaluation of Femoroacetabular Impingement and Postoperative Results

Pregraduate Research Year Thesis
Aarhus University, Health, 2016
Lars Hansen

Main supervisor:
Maiken Stilling, MD, PhD:
maiken.stilling@clin.au.dk



Preface

This thesis is based on studies performed during a pregraduate research year at the Department of Orthopaedic Research, Aarhus University Hospital, from August 2015 to August 2016.

The thesis holds an extract and supplement material. The extract is an article manuscript structured after the IMRaD model and ready for submission. The supplementary material includes a discussion of methods and sources of error, a description of studies performed and other relevant aspects.

The data and results of the research year have been presented at Congress for Pregraduate Medical research (KMS) and two different abstracts have been accepted for presentation at the congress of the Danish Orthopaedic Society (DOS) and at the annual meeting for the International Society of Hip Arthroscopy (ISHA).

Author

Lars Hansen

Department of Orthopaedic Research

Aarhus University Hospital

Tage-Hansens Gade 2, 8000 Aarhus C

Larshansen33@hotmail.com

Funding

The Novo Nordisk Foundation

The Danish Rheumatism Association

Orthopaedic Research Foundation, Aarhus

Danish Orthopaedic Society Foundation

Character count

Extract: 16,606 ; 6.9 normal pages (2400 characters per page)

Supplementary information: 29,395/ 12,2 normal pages (2400 characters per page)

Keywords

Femoroacetabular impingement, basic science, radiostereometric analysis, biomechanics, pathomechanics, arthroscopy, range of motion, hip

Acknowledgements

I would like to thank my supervisors Maiken Stilling, Sepp de Raedt, Peter Bo Jørgensen, Bjarne Mygind-Klavsen and Bart Kaptein for great support in all phases of the research year. Further I would like to thank Lars Lindgren, Lone Rømer and Lissy Fogh Kristiansen from the Department of Radiology, Aarhus University Hospital, for great contributions to data acquisition and Lone Rømer for substantial contributions to the study design. Thanks to Kirstiene Hoogeveen for graphical support, Mathias Hansen for the front page illustration and the technicians at the Technical Department, Aarhus University Hospital, for contributions to manufacturing of the setup.

List of abbreviations

dRSA	Dynamic radiostereometric analysis
FAI	Femoroacetabular impingement
ACH	Arthroscopic cheilectomy and –rim trimming
ROM	Range of motion
FADIR	Flexion, adduction and internal rotation
HRQoL	General health-related quality of life
mbRSA	Model-based radiostereometric analysis
SID	Source image distance
FSD	Focus skin distance
CE	Lateral center-edge angle

Table of Contents

Manuscript.....	7
Dynamic radiostereometric analysis for evaluation of hip joint pathomechanics....	7
Resumé.....	8
Abstract	9
Introduction	10
Materials and Methods	11
Specimens	11
Experimental setup and equipment	12
Radiographic setup.....	14
Test protocol.....	14
Analysis of radiographs.....	14
Radiation dose	15
Data analysis	15
Results.....	16
Discussion	20
Supplementary information	23
Femoroacetabular impingement	24
Project overview	25
Argumentation for choice of methods	25
Radiostereometric analysis.....	25
Radiostereometric analysis equipment (AdoraRSA)	26
Marker-based RSA and model-based RSA.....	26
Bone models.....	27
Precision and accuracy of RSA.....	28
Sources of error	28
Marker positions: distribution and stability	28
Bone models and fitting	29
Coordinate systems	29
Observer related errors.....	30
Studies performed	31

1. Donor study for validation of model-based RSA for assessment of hip joint kinematics	31
2. Donor study for evaluation of hip joint biomechanics before and after arthroscopic cheilectomy	32
3. Clinical study for evaluation of hip joint pathomechanics in FAI hips before and after arthroscopic cheilectomy	33
Statistical considerations.....	34
Methodological considerations and limitations	35
Discussion	36
Perspectives	36
Conclusions	37
References	39
Appendix.....	45
Dataset for kinematics article.....	45
Results of the kinematic study.....	46

Manuscript

**Dynamic Radiostereometric Analysis for Evaluation of Hip
Joint Pathomechanics**

Resumé

Dynamisk RSA (dRSA) muliggør non-invasiv sporing af 3D knoglebevægelser og kan benyttes til at evaluere in-vivo patologisk kinematik i hoftedeppet. For eksempel de kinematiske forhold i forbindelse med femoroacetabulær indeklemning (FAI) og de biomekaniske ændringer som keilektomi og acetabular knoglefræsning (ACH) bibringer.

Studiets formål er at evaluere de kinematiske ændringer i hoftedeppet efter ACH.

Syv hofter fra humane donorer blev CT-skannet og CT-knoglemodeller blev konstrueret. dRSA optagelser af hofterne blev rekvireret ved 5 frames/sek ved fleksion til 90°, adduktion til stop og intern rotation til stop (FADIR). ACH blev udført og dRSA gentaget. dRSA optagelserne blev analyseret vha. af model-baseret RSA (mbRSA). Hoftekinematikken før og efter ACH blev sammenlignet parvist. Volumen af reseceret knogle blev kvantificeret og sammenlignet med postoperativ bevægeomfang (ROM).

Middel intern hofterotation steg fra 19.1° til 21.9° ($p=0.04$, $\Delta 2.8^\circ$, $SD=2.7$) efter ACH. Middel præ- og postoperativ adduktion på hhv. 3.9° og 2.7° forblev uændret ($p=0.48$, $\Delta -1.2^\circ$; $SD=4.3$). Den opnåede middel fleksion før 82.4° og efter 80.8° ACH var sammenlignelige ($p=0.18$, $\Delta -1.6^\circ$, $SD=2.7$). Der blev ikke observeret nogen sammenhæng mellem volumen af reseceret knogle og postoperativ ROM.

En lille øgning i intern rotation, men ikke i adduktion, efter ACH blev observeret. Flexionsvinklerne ved FADIR blev vist at være reproducerbare. Kinematisk analyse med dRSA er en ny og klinisk anvendelig metode med god potentiale til at evaluere hoftekinematik samt kirurgiske korrektioner af hoftedeppet.

Abstract

Dynamic RSA (dRSA) enables non-invasive 3D motion-tracking of bones and may be used to evaluate in-vivo hip joint kinematics including hip pathomechanics such as femoroacetabular impingement (FAI) and the biomechanical effects of arthroscopic cheilectomy and –rim trimming (ACH).

The study aim was to evaluate the kinematic changes in the hip joint after ACH.

Seven non-FAI affected human cadaveric hips were CT-scanned and CT-bone models were created. dRSA recordings of the hip joints were acquired at 5 frames/sec during flexion to 90°, adduction to stop and internal rotation to stop (FADIR). ACH was performed and dRSA was repeated. dRSA images were analyzed using model-based RSA. Hip joint kinematics before and after ACH were compared pairwise. The volume of removed bone was quantified and compared to postoperative range of motion (ROM).

Mean hip internal rotation increased from 19.1° to 21.9° ($p=0.04$, $\Delta 2.8^\circ$, $SD=2.7$) after ACH surgery. Mean adduction of 3.9° before and 2.7° after ACH surgery was unchanged ($p=0.48$, $\Delta -1.2^\circ$; $SD=4.3$). Mean flexion angles during dRSA tests were 82.4° before and 80.8° after ACH surgery, which were similar ($p=0.18$, $\Delta -1.6^\circ$, $SD=2.7$). No correlation between volume of removed bone and ROM was observed.

A small increase in internal rotation, but not in adduction, was observed after arthroscopic cheilectomy and –rim trimming in cadaver hips. The hip flexion angle of the FADIR test was reproducible. dRSA kinematic analysis is a new and clinically applicable method with good potential to evaluate hip joint kinematics and to test FAI pathomechanics and other hip surgical corrections.

Introduction

Femoroacetabular impingement (FAI) is caused by an abnormality in the acetabular shape or orientation (Pincer-type), by a shape-abnormality in the proximal femur (Cam-type) or by a combination of the two (mixed-type) ^{1,2}. FAI most often presents in healthy, physically active, young persons (predominantly male) in the age range of 20-30 years ³. It is recognized as a common cause of pain and early development of osteoarthritis ^{4,5}. The reported prevalence of asymptomatic FAI in radiographs is 23%-32% for CAM lesions and 43%-67% for pincer lesions ^{6,7}. Studies show that physical impairments for individuals with symptomatic FAI primarily consist of motions bringing the hip towards impingement. Typically impaired daily activities are stairclimbing, squat and restrictions in frontal, transverse and sagittal hip motion during gait ^{8,9}. Further, studies have shown that FAI patients lack hip muscle strength compared to normal controls ^{10,11}.

The preferred surgical treatment of FAI is by arthroscopic cheilectomy and -rim-trimming (ACH) ¹². Excess bone is removed in the head-neck transition of the femur bone and in the anterolateral region of the acetabular rim. Arthroscopic technique is superior to an open approach based on higher postoperative general health-related quality of life (HRQoL) score ¹² and an increased patient satisfaction of 82% ¹³. Still the main reason for revision after ACH procedure is failure to identify and/or reshape the affected areas in the joint adequately ¹⁴⁻¹⁷.

Earlier studies have investigated joint kinematics related to FAI pre- and postoperatively. Simulation studies using CT-reconstructed bone models for simulation of impingement positions have been performed ¹⁸⁻²⁰. Limitations of this method are that it commonly assumes range of motion (ROM) to be governed by bone-bone contact, and they do not track the exact in vivo motions of the bone ²¹. Advantages of simulation studies are that no large setup is required and patients are only exposed to radiation in relation to the CT-scan that is used to create bone models. Motion capture systems primarily investigate functional in-vivo hip kinematics during gait or squat, but do not investigate ROM during passive movements ^{8,22,23}, subluxation of the hip joint (translation of the femur center of rotation with respect to the femur) and bone-bone distances due to soft tissue artifacts ²⁴. Kapron et al. used dual fluoroscopy and a digitally reconstructed radiograph based analysis method for tracking bone movements

during flexion, adduction and internal rotation (FADIR), and investigated in vivo kinematics of the hip joint in three FAI-patients and six non-FAI participants^{21,25}. They found that the FAI-group had decreased adduction and internal rotation during passive tests and further that ROM is governed by labrum contact and other soft tissue restraints in the native joint. They did not investigate post-operative changes in kinematics.

The pathomechanics for development of symptoms in FAI are not well understood, and neither are the kinematic changes in relation to arthroscopic surgery. In an earlier validation study we have proposed dynamic bone model-based radiostereometric analysis (mbRSA) as a method for evaluation of hip kinematics in FAI.

The aim of this study was to evaluate hip-joint kinematics in human cadaveric specimens before and after arthroscopic cheilectomy and – rim trimming.

Materials and Methods

Specimens

Eight human cadaveric legs including hip joints and hemipelvises, from 4 donors were used in the study (Department of Biomedicine, Aarhus University). One leg was excluded from the study due to a sliding hip screw, but was used for prior tests. The age of the donors ranged between 58 and 94 years, three were from male- and four from female donors. Inclusion criterion was no prior hip surgery, which was assessed by x-ray of the hip and visual inspection for earlier surgical incisions.

The donor legs were scanned in a Philips Brilliance 64 computed tomography scanner. Settings were 120 kV, 150 mAs, slice thickness 2.5 mm and slice increment 1.25 mm. Bone models were created using an automatic graph-cut segmentation method (Krčah et al. 2011, de Raedt et al. 2013). Bone segmentations of the pelvis included the iliac-, ischial- and pubic bone and for the femur the head down to 5-7 cm distally to the lesser trochanter. Local coordinate systems were created for the bone models by the method described by Baker et al.²⁸.

Experimental setup and equipment

A portable fixation for the hemipelvises which could be mounted both to the radiology table during recordings and in an operative setting during ACH was constructed (figure 1, 2, 3 and 4). Fluoroscopy was made possible from the medial side and used for entering the joint and evaluating the amount of traction applied. Traction was applied using a winch by pulling on a strap around the distal femur. ACH was performed with a 70° wide angle arthroscope, a radiofrequency wand (super multivac 50), burr (5.5 mm barrel burr) and a shaver (dyonics incisor plus), (all surgical equipment was provided by Smith and Nephew).

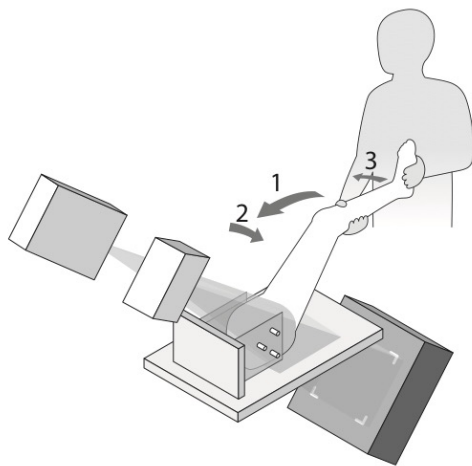


Figure 1 – Setup of the radiostereometric equipment. The x-ray tubes are positioned with 20° medio-lateral and 45° cranio-caudal tilt. The calibration box is placed in a 45° angle beneath the hip joint. The FADIR motion is indicated by the numbered arrows: 1) Flexion to 90° 2) adduction to stop 3) internal rotation to stop.

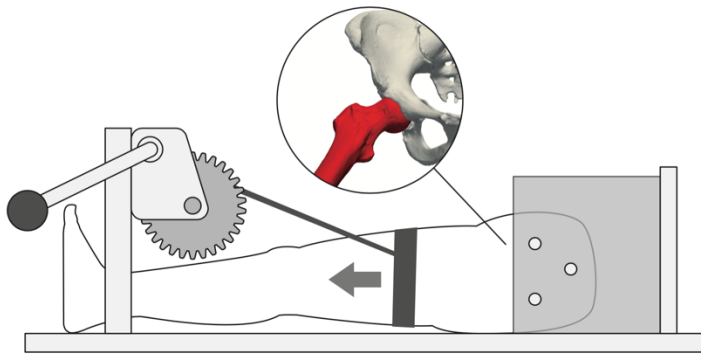


Figure 2 – The surgical setup. The pelvis was mounted in a portable fixture using three spiral drills. Traction was applied using a winch which could be adjusted in height to change flexion angles during ACH.



Figure 3 and 4 – Images of the surgical setup during ACH. The lateral portal was placed using fluoroscopic guidance.

Radiographic setup

All stereoradiographs were recorded using a dynamic RSA system (Adora RSAd, NRT X-Ray, Denmark). Sampling frequency was 5 frames/sec. Roentgen tubes were positioned with a 45° cranio-caudal- and 20° medio-lateral tilt directed at the hip joint from the cranial-caudal direction. Beneath the table a uniplanar calibration box (Box 14; Medis Specials, Leiden, the Netherlands) was placed in a 45° angle to the horizontal plane (Figure 1). The two image detectors (Canon CXDI-70C) were slotted in the calibration box. Source image distance (SID) was 2220 mm and focus skin distance (FSD) 1140 mm. Exposure settings for dRSA recordings were 130 kV, 500 mA, 16 ms and resolution was 1104x1344 pixels (79 DPI).

Test protocol

Preoperatively the cadaver specimens were CT-scanned and dRSA was performed. One dynamic RSA recording of the hip during FADIR motion, which is the movement of the donor leg from full extension through flexion to 90°, adduction to stop and internal rotation to stop (end range) was made (Figure 1). ACH was performed by the senior surgeon (BMK). Postoperatively dRSA was repeated and a postoperative CT-scan of each specimen was performed.

Analysis of radiographs

For analysis of radiographs the commercially available software model-based RSA 4.01, (RSAcore, LUMC, Leiden, The Netherlands), was used. For each specimen calibration of the image was performed in the first frame. For the mbRSA-analysis the created bone models were implemented in the program. Contours of the pelvic- and femur bones were detected on the two simultaneous images of the same scene by the Canny Edge Detector and relevant contours were manually identified, aiming to use similar contours in each frame. mbRSA automatically positions the bone models using three consecutive algorithms: IIPM, DIFDHSAnn and DIFDoNLP. These algorithms estimate the pose by minimizing error between the virtual projections of the bone models and the manually detected contours on the radiographs²⁹. For each specimen the frame in the sequence, in which the hip was in end range FADIR, was identified and

used to determine flexion, adduction and rotation angles of the hip joint along with femoral end range subluxation (the norm of translations of the femur bones' center of rotation with respect to the pelvis).

The CT-scans of the separated hemipelvises were aligned with the contralateral side to determine the anatomic coordinate system and subsequently the lateral center-edge angle (CE) and alpha angle were calculated to determine the preoperative degree of FAI by Clinical Graphics (Delft, The Netherlands).

The removed bone after ACH was determined by aligning the pre- and post-operative CT scans using image registration and segmenting the region with an intensity change above 50 Hounsfield units. The resulting model represents the post-operative bone showing the area where bone was removed during ACH. The depth of the removed bone was calculated as the distance from each point of the post-operative surface to the closest point on the pre-operative surface (Figure 5).

Radiation dose

Based on real time dRSA recordings dose-calculations were performed. The revealed effective dose per exposure was 0.054 mSv. Recordings were acquired at 5 frames/sec with a mean exposure time of 9 seconds giving an effective dose of 2.43 mSv per recording. The CT-scan contributed with an effective dose of 10 mSv per scan. Total effective dose was 24.86 mSv per specimen.

Data analysis

Data was summarized as flexion-, adduction- and internal rotation angles as measures of ROM. Two sample t-tests were used to compare pre- and postoperative results. Scatterplots of the volume of removed bone against flexion, adduction and internal rotation respectively were constructed to check for correlations. End range sub-luxation was measured as the norm of translations along the x-, y- and z-axes by use of the 3D Pythagorean theorem ($T^2 = X^2 + Y^2 + Z^2$). Pre- and postoperative sub-luxation was compared using two sample t-tests. The statistical significance level was set to 5% and Stata/IC 14.1 (StataCorp, Texas) was used for statistical analyses.

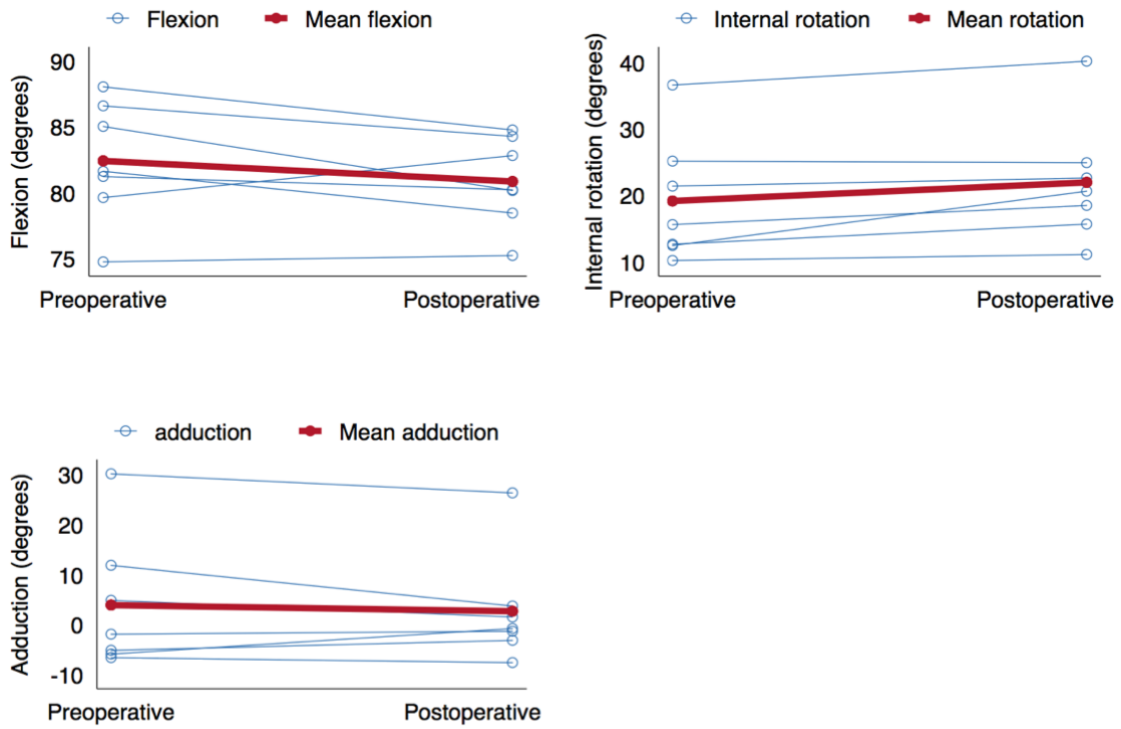
Results

The kinematic results showed a postoperative mean increase in hip rotation of 2.79° (SD=2.7; p=0.04). No increase in adduction was observed (mean difference 1.23°, SD=4.3; p=0.48) and no statistical difference in flexion was found between pre- and postoperative recordings, mean difference -1.57° (SD=2.7; p=0.18) (Graph 1). Mean pre- and postoperative flexion angles were 80.8° and 82.4° respectively. The flexion angles for the individual donors varied between 75° and 87° but no significant development from pre- to postoperative was observed (Graph 1). No correlation was found between ROM and volume of removed bone (Graph 2).

A large variation in the volume of removed bone on the femur was observed with a mean volume of 894 mm³ (SD=459 mm²) and minimum and maximum values of 335 and 1609 mm² (Table 1).

Mean pre- and postoperative subluxation (combined measure, all three axes) at end range FADIR, 3.9 and 3.5 mm respectively, did not differ significantly (SD=0.96; p=0.37). Also no differences were observed (p>0.05) when comparing the translations for the individual degrees of freedom.

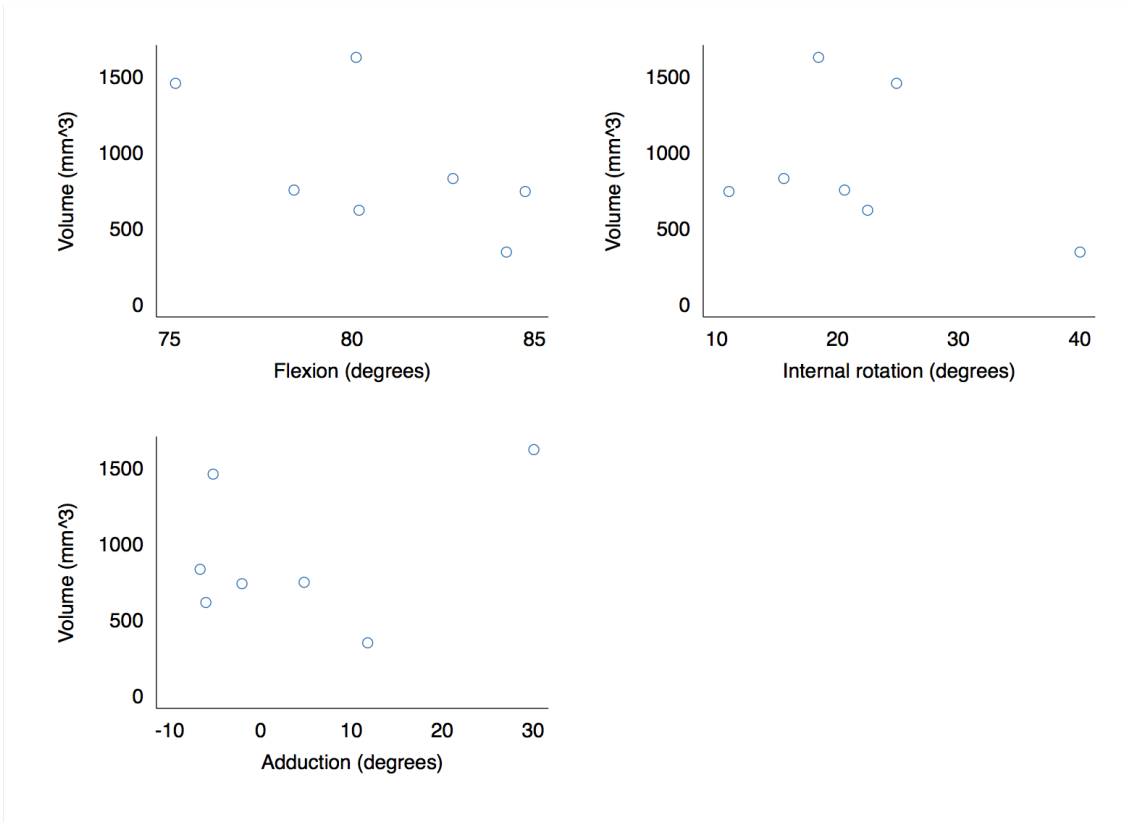
Measurements of CE and alpha-angles revealed that none of the donor hips had a cam-lesion ($\alpha < 55^\circ$) but showed that two of the donors had a CE > 40° and thereby per definition a pincer-lesion (Table 1).



Graph 1 – Scatter plot showing the development in flexion, internal rotation and adduction between the pre- and postoperative investigation.

Donor ID	CE (°)	Alpha (°)	Volume (mm ³)
1	39.5	43.0	816
2	43.1	48.3	734
3	39.2	43.4	335
4	47.4	43.2	1609
5	36.8	48.1	604
6	36.7	42.3	724
7	28.1	51.6	1439

Table 1 – Table showing the preoperative CE and alpha angle and volumes of removed bone during ACH for the seven donor hips.



Graph 2 – Scatter plots of the volume of removed bone with respect to the postoperative flexion, internal rotation and adduction.

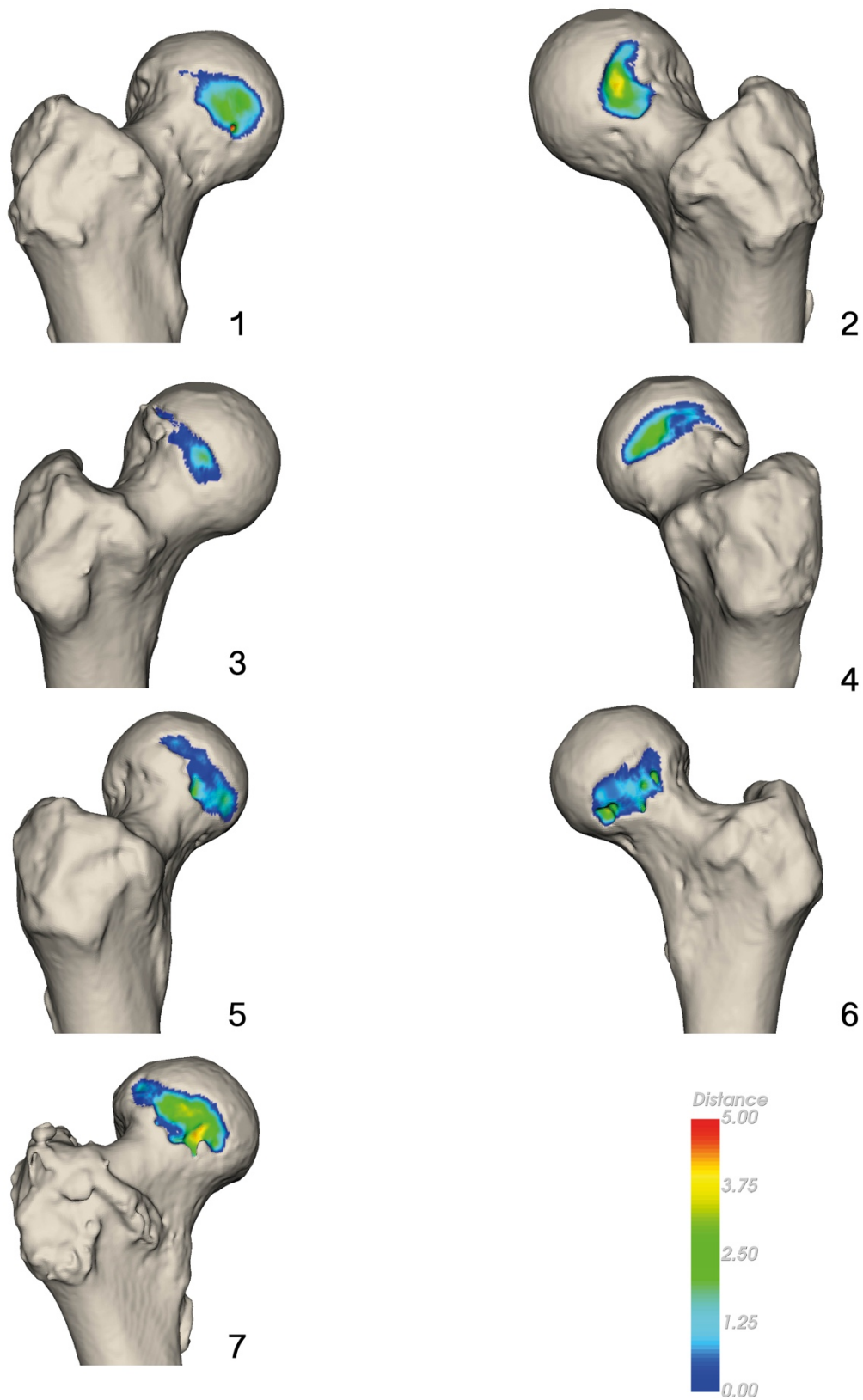


Figure 5 - Figure showing the area and depth of resected bone during ACH for all seven donor hips. The color scale refers to the depth of the resection in millimeters.

Discussion

Dynamic radiostereometry was used to investigate kinematic angles in the hip joint of human cadaver specimens during a passive FADIR motion before and after ACH, and the key finding was a small increase of 2.79° in internal rotation but no increase in adduction. The mean removed bone was 894 mm^3 .

After ACH the joint space was meticulously emptied for excess water to reduce the influence on measurements. However, the increase in internal rotation was smaller than expected and might be explained by water accumulation in the tissue around the hip causing edema and rigidity. No difference in pre-and postoperative hip joint subluxation was observed, and therefore eventual loss of muscle tone stabilization after traction on the hip joint and eventual postoperative capsule laxity after distension during arthroscopy cannot explain the small post-operative increase in hip ROM. Since flexion angles did not differ significantly, they too do not explain the low increase in internal rotation. In patients we would expect blood circulation and recovery time after surgery before control measurements would be possible to eliminate this issue and provide greater kinematic improvements after ACH.

The use of cadaver specimens makes a good imitation of the clinical situation and we have formerly shown mBRSA evaluation of hip kinematics to be very precise (submitted paper, summary in supplement material). However, there are a number of limitations in this study related to the use of cadavers. Due to the high age of specimens the bone quality was low and labrums were calcified, which made it more difficult to determine the border between the labrum and the acetabular bone on the CT-scans. Hereby, much of the labrum was segmented along with the bone during model-construction making the pelvis bone model less accurate in the acetabular rim region. Therefore, measurements of the CE angle are expected to be higher and it was not possible to measure the amount of bone removed from the acetabulum. Further, the inability to differentiate between the bone and the labrum made it impossible to measure bone-bone distances at impingement and determine whether the bones collided at end range FADIR. Further, the poor bone quality influenced the conditions for bone removal at a consistent depth because the burr would easily penetrate into the bone in soft regions. This may have contributed to the large variation between subjects in volume of removed bone.

The cadaver fixture and fixation had to allow for stereoradiography and therefore only a small area of the ilium could be used to ensure that the fixation did not block the x-rays. At end range FADIR the mean pre- and postoperative hip flexion angles were measured to be 80.8° and 82.4° with RSA, while we anticipated to reach 90° clinical flexion during testing. This may also be attributed to the use of cadaveric hemipelvises which made it more difficult to estimate the exact flexion angle during the experiment. Yet, due to the variation in pelvic tilt and the variation between patients this may also be a challenge in clinical studies. However, reproducibility to reach the same flexion position pre- and post-operative was good with a mean difference of -1.57°.

The CT-scans and RSA examinations contributed with a combined effective dose of 24.86 mSv. During the study further tests have been performed on the required quality of the CT-scans. A new CT-scanner has been installed at our institution and the field of view has been decreased to include a lesser part of the pelvis. This will allow for a substantial dose reduction of the CT-scans to 5.2 mSv for the pre- and postoperative scans respectively. The reduction in radiation dose justifies the use of mbRSA for future clinical use in FAI patients, when taking the severity and prevalence of FAI into account. Furthermore, the kinematics can be determined without the post-operative CT scan by using the models created from the pre-operative CT scan, which would further reduce the dose in clinical use. However, then no estimate of the removed bone can be calculated.

To our knowledge only one very small numbered in-vivo RSA study evaluating hip joint kinematics has formerly been conducted. Kaplan et al. used a digitally reconstructed radiograph based method for preoperative in vivo kinematic investigations of the hip on five normal subjects and three symptomatic FAI subjects. They suggested that the restriction of hip ROM is governed by the labrum and other soft tissue constraints²¹. Since only three symptomatic FAI patients were included, no statistical comparison was performed.

The pain reduction after ACH that has been reported in patients might not be caused by improved adduction and internal rotation but by a reduction in labral stress in the resected regions^{12,13}. Applying mbRSA for evaluation of FAI hips in a clinical study could provide further insight of the in-vivo pathomechanics of FAI and the mechanisms causing pain. mbRSA has proven to be an applicable tool for in-vivo bone tracking and

has potential to be used for evaluation of other corrective interventions of the hip such as periacetabular osteotomy in hip dysplasia ^{30,31}. A better understanding of the biomechanics relating to various hip conditions may improve the understanding of the etiology and thereby improvements in treatment and surgical correction.

In this study we have shown that hip internal rotation increases after ACH in cadaver hips, that flexion angles during FADIR test may be reproduced, and that the volume of removed bone on the femur can be quantified. Importantly, the study has provided valuable knowledge concerning the RSA set-up, exposure settings, CT-protocol, patient-positioning and other details needed in order to apply dynamic RSA with bone-models in clinical use for evaluation of hip kinematics. In the future, this method may provide surgeons with the necessary insight to further improve patient outcome and satisfaction when using ACH.

**Supplementary
information**

Femoroacetabular impingement

Femoroacetabular impingement (FAI) is defined as a shape abnormality in the acetabular rim (Pincer), in the head-neck transition of the femur bone (CAM) or by a combination of both (mixed type) (Figure 6)^{1,2}. FAI is common in healthy, young and physically active individuals (predominantly male), in the age range of 20-30 years. It is recognized as a common cause of pain, early development of osteoarthritis and often causes decreased range of motion (ROM).

The preferred surgical treatment of FAI is by arthroscopic cheilectomy and acetabular rim trimming^{4,5}. Excess bone is shaved off in the head-neck transition of the femur and in the anterolateral region of the acetabular rim to restore normal morphology. Arthroscopy shows higher postoperative general health-related quality of life (HRQoL) score¹² and a patient satisfaction of 82%¹³. Still the main reason for revision is

failure to identify and/or reshape the affected areas in the joint adequately¹⁴.

Only few studies have investigated the pathomechanics of FAI, and to our knowledge only one in-vivo using dual fluoroscopy exists²¹. Kapron et al. investigated the hip arthrokinematics of three symptomatic FAI patients and six non-FAI participants by use of dual fluoroscopy during FADIR (Flexion-Adduction-Internal-Rotation test). Bone models were fitted to the recordings by a digitally reconstructed radiograph (DRR) based method. They found that the FAI-group had decreased adduction and internal rotation and that labrum contact and other soft tissue constraints limits ROM. Kinematic computer simulation studies have been performed by use of CT reconstructed bone models^{18,19,32}. Though, these assume ROM to be governed by bone-bone contact and do not take soft tissue and labrum constraints into account which have been shown to govern ROM²¹. The advantages of using simulations for identification of impingement areas are that it does not require a large setup, it is fast and the patient is only exposed to roentgen to produce the CT-scan. Studies using motion capture systems during gait have been performed^{8,22,23}. These studies primarily investigate the functional in vivo values during gait or squat and do not investigate ROM with passive movement of the

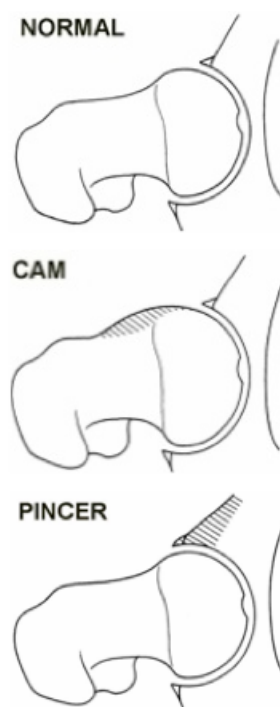


Figure 6 – FAI subtypes

hip. Hereby, gait studies give valuable information on the functional abilities of the joint whereas bone-bone distances and translations during impingement cannot be measured. Studies on knee kinematics show that motion capture systems are subject to large errors due to skin motion artifacts³³⁻³⁵. The major advantages of this method are that it is noninvasive and that the patient is not exposed to any radiation.

The aim of the research year was to understand in vivo FAI pathomechanics and the biomechanical effects of the arthroscopic treatment. With this new knowledge we hope to be able to improve treatment.

Project overview

The studies of the research year focused on a non-invasive in-vivo model-based RSA method for objective measurements of hip arthrokinematics that could be utilized both before and after surgery. In the first study, the precision of model-based RSA was validated against traditional marker-based RSA for kinematic analysis of the hip joint. In the second study, the effect of arthroscopic bone resection on hip arthrokinematics was tested in a before-and-after study on human cadaver hips by use of model-based RSA. In the third study, the effect of arthroscopic bone resection on hip arthrokinematics was investigated clinically in FAI patients before and 3 months after surgery by use of model-based RSA (the study is ongoing, 1 patient was evaluated for the research year report).

Argumentation for choice of methods

Radiostereometric analysis

Radiostereometric analysis (RSA) was introduced in 1974 by Goran Selvik³⁶, and is a highly accurate and precise method for three-dimensional tracking of objects based on calibrated dual roentgen images (stereo radiographs). RSA has been widely used for detection of migration and micromotion of implants, relative to bead-markers inserted in the bone³⁶⁻⁴⁰. Markerless methods for analysis of stereoradiographs by use of CAD or reversed engineered models of implants alleviate the need for bone-markers at the expense of precision^{41,42}. The markerless method may also use CT-reconstructed bone models, which makes the method feasible for noninvasive investigation of kinematics in native joints.

Radiostereometric analysis equipment (AdoraRSA)

The equipment consists of two x-ray tubes fixed in a rail system with auto-positioning applications. The set-up is flexible for loaded/standing and supine motion recordings. Under the investigated area, e.g. the hip joint, a calibration box is placed. The calibration box consists of a top- and bottom layer of tantalum beads – the control and fiducial markers respectively (Figure 1)⁴³. Dynamic detectors (Canon CXDI-70C detectors) are inserted into the calibration box beneath the layer of fiducial markers. Based on the known grid of tantalum markers in the calibration box and identification of the markers on the stereo radiographs it is possible to calculate the roentgen foci points and the position of the imaged object⁴⁴. The setup is applicable for both static- and dynamic recordings. With static RSA the imaged object is kept still and one frame is recorded. Under dynamic RSA a motion is recorded at a frame rate between five and 30 frames/sec.

Marker-based RSA and model-based RSA

Analysis of radiostereometric radiographs may be marker based RSA (Marker Method: MM) or model-based RSA (Model-Based Method: MBM). Analysis based on markers inserted in the bone during surgery and mounted on the implants is the original method introduced to measure micromotions of implants over 40 years ago (Gör. Selvik, 1989). The 3D-markerpositions are reconstructed from the stereoradiographs and micromotions are measured as the relative difference between the marker patterns.

With more advanced computer software techniques MBM was introduced as a method for tracking prosthetic motions based on implant models from computer-aided design (CAD) models. Advantages, compared to conventional MM, are that the implants do not need to be modified with markers, no extra sterilization of the implants is needed, and there is no risk for occluded implant markers in the images – however bead-marking of the bone is still needed as a reference object. Model-based analysis can also be used with bone models thereby optioning a noninvasive method of kinematic analysis of native joints.

The bone models may be reconstructed from computed tomography (CT) scans and fitted to manually detected bone contours in the stereoradiographs (figure 8).

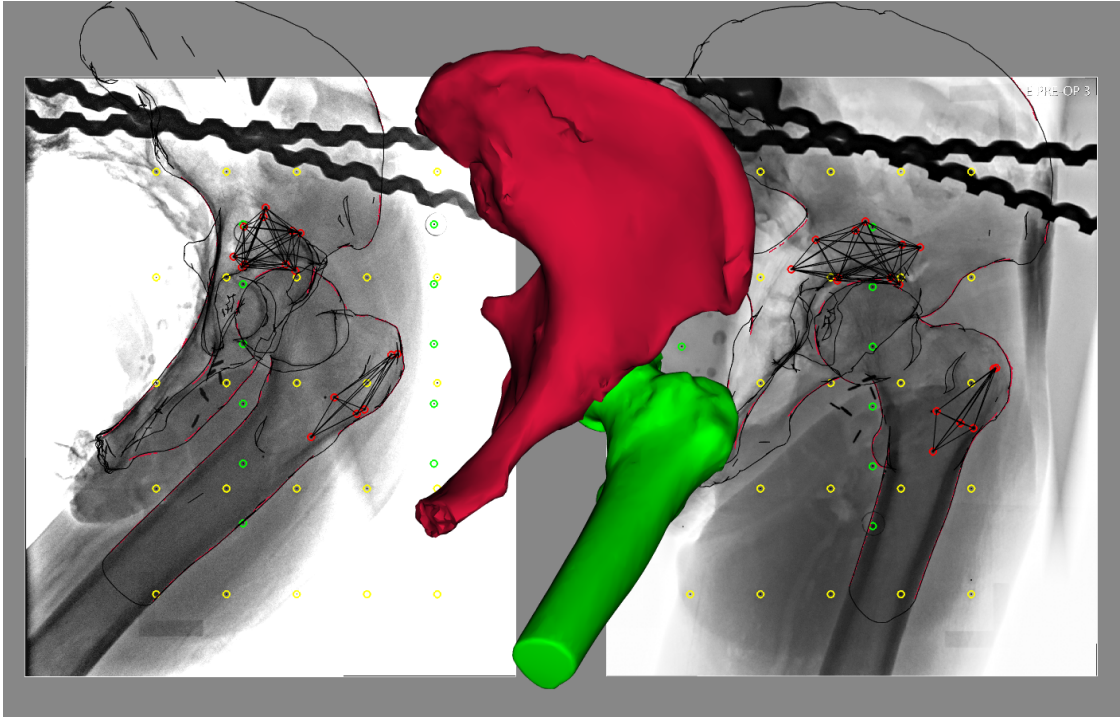


Figure 8 - Analysis of RSA images in MBRSA. The contours in the image are detected by the Canny edge detector and contours were manually selected from these (red lines indicate the selected contours). The bone models are fitted to these contours by matching their projections.

Bone models

Patient specific bone models are created from computed tomography (CT) images. First, the bones are identified by segmentation using a fully automated graph-cut segmentation method²⁶. Subsequently, the bone models are created and post-processed for compatibility with the MBM software. The models are matched with the radiographic contours of the hip in sequential stereoradiographs and measures of joint motion and congruency as well as bone contact or distance may then be calculated.

For all the bone models coordinate systems were created following the ISB recommendations²⁸. The cadaveric hips for the donor study were delivered as hemipelvises (necessary for storing options) and therefore it was necessary to simulate a full pelvis by combining the corresponding models of the hemipelvis (eight hips from four donors were acquired, one hip was excluded from the study due to an inserted dynamic hip screw, though a bone model of the pelvis was still created). Hereby it was possible to identify the corresponding landmarks that define the axes of the coordinate system.

Precision and accuracy of RSA

Measurement errors are divided into random and systematic errors. A random error is an unpredictable fluctuation in the system and the values of the error usually follows a normal distribution. A systematic error, or the bias of the technique, depends on the observer, the instrument or the technique. It can be constant or vary as a function of the measurement⁴⁵. This means that if no bias is assumed, the data will not be skewed and the mean of the random error will be zero.

The accuracy of RSA is determined as the migration- and rotational errors for all six degrees of freedom reported in millimeters and in degrees compared to the true migration, which may only be determined by comparison with more accurate methods such as object motion by micrometer screws⁴⁶. On the other hand, the precision of an RSA setup is synonymous with repeatability and may be evaluated by double examinations⁴³.

Sources of error

Marker positions: distribution and stability

The marker beads function as rigid well-defined landmarks for the analysis³⁸.

A minimum of three beads are required for tracking of the 3D-marker-positions⁴⁷ but accuracy of the analysis increases with the number of detected markers and their proper/widespread distribution (large geometrical marker matrix and less risk of markers occluding each other)^{43,48}.

The stability of the inserted markers is assessed with the mean error of the rigid body matching (ME). The ME describes the mean difference in relative distances between markers within the imaged object between RSA images. In dynamic RSA ME is measured for consecutive scenes using the previous image-scene as reference. The suggested upper limit of ME is 0.35 mm⁴³.

The distribution of markers is described by the condition number. The condition number is mathematically computed from the geometry of the matrix defined by the markers. A high condition number (CN) indicates poor distribution whereas a low

condition number indicates proper distribution⁴³. Studies have shown that analyses with condition numbers below 100-110 provide very reliable results^{43,48}.

In the current donor study the mean and maximum values for both ME and CN were substantially lower than the recommended limits indicating high quality of analyses.

Bone models and fitting

Many factors can influence the precision of MBM analyses using bone models. Factors with largest influence are bone quality, soft tissue thickness, the pose of the bone, tube angulation, image quality, and the quality of the bone models.

The CT constructed bone models are created by segmentation. When segmenting CT-scans the whole bone is segmented and the constructed model represents the actual size of the bone. In contrary, when taking x-ray images of bone, the rays must travel through a certain amount of bone before contrast is seen on the radiograph. Therefore the strongest edge lies a small distance inside the projected intensities. To account for this the analysis software Modelbased RSA (RSAcore, Leiden) allows downscaling the bone model (most frequently by 1-2%) in order to gain a more correct fit. The distance between the actual- and recorded contour might also differ throughout the imaged bone due to differences in cortical bone thickness.

The finite resolution of the CT-scans will influence the error of the constructed bone model. The scan is imaged with voxels (three dimensional pixels). The actual detected contours will lie within a voxel, and therefore the error of the bone model varies with resolution. Ultimately, resolution influences the fit of the model in the analysis, and a high CT scan-resolution increases model accuracy.

To ensure the lowest rotational errors when fitting bone models in MBM it is important to use identifiable contours with the largest possible geometrical distance apart. Further, fitting of symmetrical objects and long slim objects (such as the femur) has a large influence on rotation error. This is also clear in the current study where Y-rotation error for the femur bone is larger than for the pelvis.

Coordinate systems

In radiostereometry two different coordinate systems can be used to describe the migration of the imaged object, a local- and a global coordinate system. The calibration

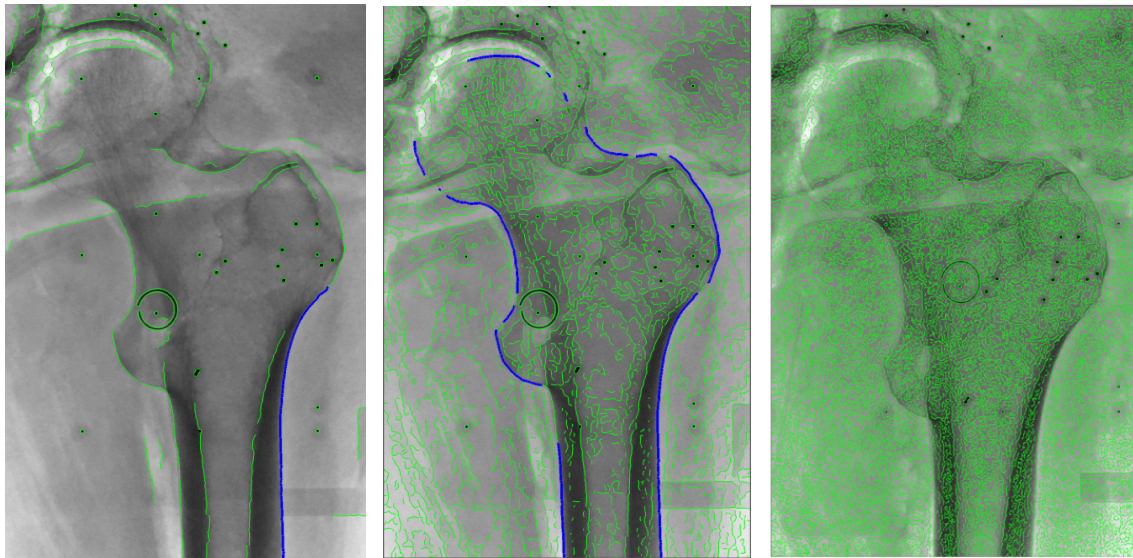
box defines the global coordinate system. The position of the imaged object within the global coordinate system will differ between recordings, as positioning cannot be reproduced exactly. These differences are accounted for by transformations^{48,49}. Local coordinate systems are defined within the reconstructed bone models and define the orientation of the model. For the hip joint both the pelvic- and the femoral coordinate systems originate in the hip center of rotation (HCR). Several algorithms can be used to calculate HCR⁵⁰. Stagni et al.⁵¹ have shown that inaccuracies in the estimation of HCR ultimately affects calculations of angles and thereby the accuracy of the kinematic analysis. In the current study it was necessary to graphically simulate a complete pelvis by connecting the CT models of the corresponding donor hemipelvises. This was done with care but might give origin to some error.

Observer related errors

Model-based RSA (MBRSA, RSAcore, Leiden) is semi-automated computer analysis software for radiostereometric images, which limits the number and impact of observer related errors⁵². Still, several of the automated processes require the user to adjust settings which ultimately can lead to improper use. Hence, systematic training and user experience are prerequisites for performing proper analyses.

Detection of markers is automated but requires the user to change threshold settings. The user must be aware to standardize these settings as improper marker detection will lead to incorrect calibration of recordings and ultimately lower the measurement accuracy.

This is also the case when detecting bone contours for model-based analysis (adjustment of threshold settings), and in the current study identical threshold settings were used for all radiostereometric images (smooth: 4 px; Threshold: 100). Figure 9 shows the effect of change in “threshold” and “smooth” elicits on the contour detection. Accurate and precise detection of bone contours and markers depends on image quality for the user to be able to identify the correct contours. Amongst factors influencing on image quality are bone quality, contrast, exposure and resolution.



Smooth: 4 px
Threshold: 500

Smooth: 4 px
Threshold: 100

Smooth: 2 px
Threshold: 100

Figure 9 – The effects of changing the smooth and threshold of the contours detected by the Canny edge detector.

Studies performed

1. Donor study for validation of model-based RSA for assessment of hip joint kinematics

Many factors can influence on the quality of dynamic RSA, hereunder the RSA setup, speed of the recorded object, amount of soft tissue etc. Only one other study, with a low number of subjects, investigates hip kinematics by dynamic RSA, but with a different RSA system, and therefore a donor study was needed in order to establish the precision and feasibility of dynamic RSA setup and bone model method with traditional marker-based RSA as the gold standard^{21,25}. Initially various setups using different calibration boxes were tested, and the final setup was chosen based on image quality (detectable contours, clear image through the motion, largest parts of the imaged bones) and clinical feasibility (easy to set up equipment and position patient, good image quality during motion). The following is a brief description of results and a discussion about choice of methods.

Results

In the validation of MBM systematic error was approximately zero in translations (mean diff < .014mm) and rotations (mean diff < 0.009°). Precision assessed as limits of agreement (LoA = mean +/- 1.96*standard deviation) was up to 0.5° for rotations and

0.5 mm for translations. LoA for translations of the femur ranged between 0.15 and 0.44 mm (min and max errors: -0.83 and 0.67 mm), for the pelvis between 0.21 and 0.91 mm (min and max errors: -1.5 and 1.9 mm). LoA for femur rotations ranged between 0.37 ° and 0.71° (min and max error: -1.6° and 1.3°) for the pelvis between 0.48° and 0.58°(min and max error: -1.2° and 1.4°). Largest rotation errors were observed for the y-rotation of femur, for translations the largest errors were observed along the z-axis (see results in the appendix under “Results of the kinematic study”).

In the current donor study the mean ME was 0.0629 mm (95% CI 0.0593; 0.0665, min=0.0139 mm, max=0.202 mm) and the mean CN was 33.7 (95% CI 32.6; 34.7; min=15.0, max=51.5). Substantially lower than the recommended highest values.

Discussion

The aim was to validate MBM as a tool for evaluation of hip joint pathomechanics with MM as the gold standard in non-FAI affected human cadaveric hips. MBM was concluded applicable for clinical use of hip joint biomechanics with acceptance of a mean difference <.014 mm for translations and <0.009° for rotations in comparison with MM and a precision well above 0.71° and 0.9 mm. Further, the setup was applicable for a clinical study. High resolution CT-scans were used why the bone models should be accurate. The purchase of a new CT-scanner has made it possible to produce high resolution scans with substantially reduced dose exposure which will be used for the clinical study.

Further, the method can be used to evaluate hip joint biomechanics through measurements of ROM and bone-bone distances.

2. Donor study for evaluation of hip joint biomechanics before and after arthroscopic cheilectomy

Changes in hip joint arthrokinematics are difficult to assess precisely in vivo with dynamic methods and only one other small scale RSA study has been performed and used different systems, models and set-up. This study aimed to evaluate hip joint biomechanics before and after arthroscopic cheilectomy in native cadaver hip joints. It is the main body of the research year thesis and is presented in detail in the article manuscript (dataset available in the appendix under “Dataset for kinematics article”).

3. Clinical study for evaluation of hip joint pathomechanics in FAI hips before and after arthroscopic cheilectomy

Little is known about the pathomechanics of in vivo FAI and about the kinematic changes brought by the arthroscopic treatment of FAI. Therefore a clinical study was initiated using the validated MBM method. Patient inclusion was delayed several times during the research year, but the first patients were operated in June 2016. Results are unfortunately not available for reporting in this thesis.

Materials and methods

The test protocol for the clinical study is similar to study 2 except that pain on VAS is also registered during tests. Patients diagnosed with FAI are being included. At a planned preoperative examination patients are CT-scanned and dynamic RSA of the hip is performed. During RSA the hip will be flexed to approximately 90 degrees, dRSA recording is started and the hip is then adducted and internally rotated three times (end-range FADIR) after which the recording will stop. Arthroscopic cheilectomy and -rim trimming is performed approximately two weeks after preoperative RSA and -CT. Three months postoperatively radiology is repeated. Further RSA recordings are performed at one, two and five year FU. Additional CT-scans may be performed on clinical indication.

Argumentation for change in RSA-protocol

Based on experiences from the donor study and ethical considerations (x-ray dose reduction) the RSA-protocol for the clinical study differs from the donor study since recordings are solely being performed in the near and end of FADIR motion (motions stops when the patient experience pain or a mechanical stop). In all other aspects the setup and x-ray settings are identical to that of the donor study.

Inclusion of patients and ethical considerations

The study has been reported to and approved by The Central Denmark Region Committees on Health Research Ethics and the Danish Data Protection Agency. Patients are being included in the study by a senior sports medicine consultant (BMK)

in the Department of Orthopedic Surgery, Aarhus University Hospital. Oral and written study material is provided, and patients must sign a consent form. The instruction from the Helsinki II declaration is followed. Care has been taken to plan all possible research related investigations together with other hospital visits according to normal hip arthroscopy protocol. No similar study has been performed why it was not possible to perform a power calculation. Based on experience from earlier studies in the group it was decided that 25 patients were included.

Dose-risk assessments of dynamic RSA performed on hip patients revealed an effective dose for one dynamic recording of 2.43 mSv (exposure time: 9 sec; 5 frames/sec) (ICRP 103). Total effective dose of five RSA recordings during the study contribute with 12.15 mSv. The pre- and postoperative CT-scans contribute with an effective dose of 5.2 mSv. Hereby participants in the study will receive a total of 22.5 mSv. In perspective, the annual effective dose received from background radiation in Denmark is 3 mSv. Hence, the effective dose patients will receive in the study is equal to seven years of background radiation. For participants under 50 years of age, participation will contribute with an estimated greater risk of death by cancer of 10^{-3} or greater. This should be added to the cancer mortality for other causes, not related to this exposure, which in Denmark is of 25 %⁵³.

Statistical considerations

For the validation study the migration data obtained consisted of the migration error (mm) and rotation error (degrees) in all six degrees of freedom of MBM with respect to MM as gold standard. Migratory data were summarized as means, standard deviation (SD), limit of agreement (LoA) and minimum and maximum value. The mean of the observations represents the systematic error of the method. T-tests were used to test if the means differed significantly from zero. Precision was assessed as the variance of the migration results. Variance was calculated as limits of agreement (LoA) (LoA=1.96*SD) and prediction intervals (PI) (PI=1.96*SD±mean).

ME and condition number were summarized by means and minimum and maximum values to evaluate the quality of the MM-analysis³⁸.

Methodological considerations and limitations

The MBM method is accurate and precise but analysis intensive with requirement of manual analysis of all stereoradiographs. dRSA of one FADIR hip exercise produces many images for each analysis (approximately 25) and analysis time per image is approximately 15 min. This limits the application of the method primarily to research use. Expansion of dRSA for evaluation of joint kinematics in general would require development of a more automated analysis method that can make analyses/results readily available and easy to acquire.

MBM exceeds the clinically relevant precision for measurement of flexion-, adduction- and internal rotation angles. As accuracy is not investigated in this study it is not possible to determine if accuracy is high enough to measure clinically relevant bone-bone distances at end range FADIR. Though, if the variation in bone-bone distance determined from the clinical study exceeds the precision of MBM it will be possible to measure these.

The primary strength of the study setup is that it permits RSA recordings of the hip joint in the position of a clinical diagnostic test (FADIR), however the x-rays must pass through much tissue. Therefore, patient obesity will influence image quality and potentially the quality of the analysis. This can be compensated for by adjusting the exposure settings during dRSA.

The pre- and postoperative radiological examination of the hips expose the patients to a quite large radiation dose (22.5 mSv). However, due to the severe functional limitations and pain that FAI cause in patients, and the limited knowledge about the effect of arthroscopic treatment, the Ethics committee found that it was justified to perform the study. Still, the relatively high radiation dose from CT-scans for development of personal bone models of the femur and pelvis, limits a wide clinical application until other methods that reduce radiation dose, e.g. magnetic resonance imaging reconstructed bone models or statistical shape bone models, have been developed. Alternatively, low dose CT scans may also be used after validation of model quality. Cone Beam CT is another low radiation dose 3D model method, however not feasible for the hip joint due to the small gantry in the scanner. Eventually, MBM might not be part of a standard clinical diagnostic procedure but could be used for extraordinary

cases or for patients who continue to experience pain, where it would be relevant to know more about hip joint kinematics.

Discussion

During the research year the precision of MBM has been validated against gold standard MM, and the kinematic changes in the hip joints after arthroscopic cheilectomy has been established in a donor study of native human hips by use of MBM. The MBM method was concluded valid for clinical use with a precision well above (0.7° and 0.9 mm) any other available non-invasive kinematic analysis method. The strengths of the MBM method are that the method is non-invasive (no surgery required), the FADIR motion could be reproduced well, and all in vivo structures surrounding the joint may be kept intact. Therefore, the method is ideal for clinical use in pre- and postoperative evaluation of hip joint kinematics, and may potentially be used in several different clinical hip studies of pathomechanics i.e. FAI, dysplasia, osteoarthritis, calve-perthes etc. A limitation in the donor setup is that water seems to accumulate in the tissue after arthroscopy causing edema and rigidity. This will to some extent affect the kinematic measurements of the study making definite conclusions about the kinematic effects of arthroscopic cheilectomy and -rim trimming a bit uncertain. Other weaknesses are that the method with the currently available radiological techniques expose the typical mid-age patients to a relatively high radiation dose, and image analysis is quite time consuming.

The design of the clinical study is strong regarding the ability to combine biomechanical analyses with PROMs in a longer term follow-up. Further the combined methods and set-up has the potential to investigate correlations between changes in adduction and rotation angles, regrowth of pincer and CAM bone, and bone-bone distances at presumed impingement (pain). The major weakness of the study is lack of controls, which naturally would never be feasible from a research ethical point of view, due to the high radiation dose (CT).

Perspectives

There are many interesting perspectives of the results obtained through out the research year. MBM was validated as a highly accurate and precise method in comparison with gold standard MM, and further it is a noninvasive method for evaluating hip joint

kinematics. Potentially, MBM can provide valuable precise quantitative information on hip joint kinematics in various hip conditions, but the purpose of the current study was to evaluate a new method that may help gain information about arthroscopic treatment of FAI. After completion of the clinical study and a dynamic RSA FAI database, MBM may possibly also be used as a diagnostic tool in hip pathomechanics, help surgeons in the determination of which patients may benefit from surgery and which may not, and further help the hip surgeon develop more effective treatments for different hip conditions. In our group, MBM has already been used in a kinematic study on the knee and it is process of being validated for many other joints. Currently there is focus and efforts in our research group on development of a fully automated analysis method for dynamic RSA, which could decrease the amount of man-hours spent on analysis and thereby widen the clinical applicability. Furthermore, studies are being performed on creating bone models from MRI-scans. If these can be produced with equal precision to CT-reconstructed models the clinical potential would be even greater due to lower radiation dose.

The cohort that is being built up during the clinical study is unique and will allow for additional sub-studies. At longer term follow-up it would be relevant to evaluate if regrowth of the cam- and pincer bone lesions occurs, PROMs in relation to kinematic results, changes in hip kinematics over time e.g. does regrowth happen and does it cause a renewed reduction in ROM or does tightening of the joint capsule or other formations of scar tissue cause kinematic changes over time. Further evaluation of kinematic factors (e.g. large/low restrictions of ROM, large/low bone translations at impingement) that may be predictive of outcome at the end of FU (five years) are planned.

Conclusions

In summary, the results produced during the research year has provided clinicians and researchers in our institution with an accurate, validated non-invasive and precise method for tracking the bones in the hip joint. The clinical applicability for kinematic evaluation of arthroscopic cheilectomy and –rim trimming on normal hip joints were tested in a cadaver study on human donor hips and found to be feasible and precise. Finally, a clinical study on FAI hips was designed, initiated and will continue with establishment of the worlds' first clinical database on a FAI cohort investigated with

dynamic RSA pre- and post-operatively. The first RSA recordings of these clinical patients have been analyzed and quality has proven to be high.

To conclude on my own behalf, I have gained invaluable research experience and network connections from which I can benefit throughout the rest of my medical career.

References

1. Agricola R, Waarsing JH, Arden NK, et al. Cam impingement of the hip--a risk factor for hip osteoarthritis. *Nat Rev Rheumatol*. 2013;9(10):630-634. doi:10.1038/nrrheum.2013.114.
2. Beck M, Kalhor M, Leunig M, Ganz R. Hip morphology influences the pattern of damage to the acetabular cartilage: femoroacetabular impingement as a cause of early osteoarthritis of the hip. *J Bone Joint Surg Br*. 2005;87:1012-1018. doi:10.1302/0301-620X.87B7.15203.
3. Ganz R, Parvizi J, Beck M, Leunig M, Nötzli H, Siebenrock K a. Femoroacetabular impingement: a cause for osteoarthritis of the hip. *Clin Orthop Relat Res*. 2003;(417):112-120. doi:10.1097/01.blo.0000096804.78689.c2.
4. Larson CM, Kelly BT, Bhandari M, et al. Impingement. *Arthrosc J Arthrosc Relat Surg*. 2016;32(1):177-189. doi:10.1016/j.arthro.2015.10.010.
5. Kowalczyk M, Yeung M, Simunovic N, Ayeni OR. Does Femoroacetabular Impingement Contribute to the Development of Hip Osteoarthritis ? A Systematic Review. 2015;23(4):174-179.
6. Frank JM, Harris JD, Erickson BJ, et al. Prevalence of Femoroacetabular Impingement Imaging Findings in Asymptomatic Volunteers: A Systematic Review. *Arthroscopy*. 2015;31(6):1199-1204. doi:10.1016/j.arthro.2014.11.042.
7. Diesel CV, Ribeiro TA, Scheidt RB, De Souza Macedo CA, Galia CR. The prevalence of femoroacetabular impingement in radiographs of asymptomatic subjects: A cross-sectional study. *HIP Int*. 2015;25(3):258-263. doi:10.5301/hipint.5000250.
8. Diamond LE, Wrigley T V., Bennell KL, Hinman RS, O'Donnell J, Hodges PW. Hip joint biomechanics during gait in people with and without symptomatic femoroacetabular impingement. *Gait Posture*. 2015;43:198-203. doi:10.1016/j.gaitpost.2015.09.023.
9. Diamond LE, Dobson FL, Bennell KL, Wrigley T V, Hodges PW, Hinman RS. Physical impairments and activity limitations in people with femoroacetabular impingement: a systematic review. *Br J Sports Med*. 2015;49(4):230-242. doi:10.1136/bjsports-2013-093340.

10. Casartelli NC, Maffiuletti N a., Item-Glatthorn JF, et al. Hip muscle weakness in patients with symptomatic femoroacetabular impingement. *Osteoarthr Cartil.* 2011;19:816-821. doi:10.1016/j.joca.2011.04.001.
11. Freke MD, Kemp J, Svege I, Risberg MA, Semciw A, Crossley KM. Physical impairments in symptomatic femoroacetabular impingement : a systematic review of the evidence. 2016:1-19. doi:10.1136/bjsports-2016-096152.
12. Nwachukwu BU, Rebolledo BJ, McCormick F, Rosas S, Harris JD, Kelly BT. Arthroscopic Versus Open Treatment of Femoroacetabular Impingement: A Systematic Review of Medium- to Long-Term Outcomes. *Am J Sports Med.* 2015. doi:10.1177/0363546515587719.
13. Sansone M, Ahldén M, Jónasson P, et al. Outcome after hip arthroscopy for femoroacetabular impingement in 289 patients with minimum 2-year follow-up. *Scand J Med Sci Sports.* 2016:n/a-n/a. doi:10.1111/sms.12641.
14. Heyworth BE, Shindle MK, Voos JE, Rudzki JR, Kelly BT. Radiologic and Intraoperative Findings in Revision Hip Arthroscopy. *Arthrosc - J Arthrosc Relat Surg.* 2007;23(12):1295-1302. doi:10.1016/j.arthro.2007.09.015.
15. Ross JR, Larson CM, Adeoyo O, Kelly BT, Bedi A. Residual Deformity Is the Most Common Reason for Revision Hip Arthroscopy: A Three-dimensional CT Study. *Clin Orthop Relat Res.* 2014:1388-1395. doi:10.1007/s11999-014-4069-9.
16. Philippon MJ, Schenker ML, Briggs KK, Kuppersmith DA, Maxwell RB, Stubbs AJ. Revision hip arthroscopy. *Am J Sport Med.* 2007;35(11):1918-1921. doi:10.1177/0363546507305097.
17. Larson CM, Giveans MR, Samuelson KM, Stone RM, Bedi A. Arthroscopic Hip Revision Surgery for Residual Femoroacetabular Impingement (FAI): Surgical Outcomes Compared With a Matched Cohort After Primary Arthroscopic FAI Correction. *Am J Sports Med.* 2014;42(8):1785-1790. doi:10.1177/0363546514534181.
18. Bedi A, Dolan M, Hetsroni I, et al. Surgical Treatment of Femoroacetabular Impingement Improves Hip Kinematics. *Am J Sports Med.* 2011;39(Supplement 1):43S-49S. doi:10.1177/0363546511414635.
19. Kubiak-Langer M, Tannast M, Murphy SB, Siebenrock K a, Langlotz F. Range of motion in anterior femoroacetabular impingement. *Clin Orthop Relat Res.*

- 2007;458(458):117-124. doi:10.1097/BLO.0b013e318031c595.
20. Sampson JD, Safran MR. Biomechanical Implications of Corrective Surgery for FAI : An Evidence-based Review. *Sport Med Arthrosc.* 2015;23(4):169-173.
 21. Kapron AL, Aoki SK, Peters CL, Anderson AE. In-vivo hip arthrokinematics during supine clinical exams: Application to the study of femoroacetabular impingement. *J Biomech.* 2015;48(11):1-8. doi:10.1016/j.jbiomech.2015.04.022.
 22. Brisson N, Lamontagne M, Kennedy MJ, Beaulé PE. The effects of cam femoroacetabular impingement corrective surgery on lower-extremity gait biomechanics. *Gait Posture.* 2013;37:258-263. doi:10.1016/j.gaitpost.2012.07.016.
 23. Rylander JH, Shu B, Andriacchi TP, Safran MR. Preoperative and postoperative sagittal plane hip kinematics in patients with femoroacetabular impingement during level walking. *Am J Sports Med.* 2011;39 Suppl:36S-42S. doi:10.1177/0363546511413993.
 24. Taylor WR, Ehrig RM, Duda GN, Schell H, Seebeck P, Heller MO. On the influence of soft tissue coverage in the determination of bone kinematics using skin markers. *J Orthop Res.* 2005;23(4):726-734. doi:10.1016/j.orthres.2005.02.006.
 25. Kapron AL, Aoki SK, Peters CL, et al. Accuracy and feasibility of dual fluoroscopy and model-based tracking to quantify in vivo hip kinematics during clinical exams. *J Appl Biomech.* 2014;30(3):461-470. doi:10.1123/jab.2013-0112.
 26. Krčah M, Székely G, Blanc R. Fully automatic and fast segmentation of the femur bone from 3D-CT images with no shape prior. *Proc - Int Symp Biomed Imaging.* 2011:2087-2090. doi:10.1109/ISBI.2011.5872823.
 27. de Raedt S, Mechlenburg I, Stilling M, Rømer L, Søballe K, de Bruijne M. Automated measurement of diagnostic angles for hip dysplasia. *SPIE Med Imaging.* 2013;8670:1-10. doi:10.1117/12.2007599.
 28. Baker R. ISB recommendation on definition of joint coordinate systems for the reporting of human joint motion—part I: ankle, hip and spine. *J Biomech.* 2003;36(1):300–302. doi:10.1080/13518040701205365.
 29. Kaptein BL, Valstar ER, Stoel BC, Rozing PM, Reiber JHC. Evaluation of three

- pose estimation algorithms for model-based roentgen stereophotogrammetric analysis. *Proc Inst Mech Eng H*. 2004;218(4):231-238.
doi:10.1243/0954411041561036.
30. Liu L, Ecker T, Xie L, Schumann S, Siebenrock K, Zheng G. Biomechanical validation of computer assisted planning of periacetabular osteotomy: A preliminary study based on finite element analysis. *Med Eng Phys*. 2015;37(12):1169-1173. doi:10.1016/j.medengphy.2015.09.002.
 31. Murphy RJ, Armiger RS, Lepistö J, Mears SC, Taylor RH, Armand M. Clinical evaluation of a biomechanical guidance system for periacetabular osteotomy. *J Orthop Surg Res*. 2016;10(4):497-508. doi:10.1007/s11548-014-1116-7.
 32. Sampson JD, Safran MR. Biomechanical implications of corrective surgery for FAI: An evidence-based review. *Sport Med Arthrosc*. 2015;23(4):169-173.
<http://www.embase.com/search/results?subaction=viewrecord&from=export&id=L606934957>.
 33. Benoit DL, Ramsey DK, Lamontagne M, Xu L, Wretenberg P, Renström P. Effect of skin movement artifact on knee kinematics during gait and cutting motions measured in vivo. *Gait Posture*. 2006;24(2):152-164.
doi:10.1016/j.gaitpost.2005.04.012.
 34. Stagni R, Fantozzi S, Cappello A, Leardini A. Quantification of soft tissue artefact in motion analysis by combining 3D fluoroscopy and stereophotogrammetry: a study on two subjects. *Clin Biomech*. 2005;20(3):320-329. doi:10.1016/j.clinbiomech.2004.11.012.
 35. Garling EH, Kaptein BL, Mertens B, et al. Soft-tissue artefact assessment during step-up using fluoroscopy and skin-mounted markers (Journal of Biomechanics (2007) 40, SUPPL. 1, (S18-S24) DOI: 10.1016/j.jbiomech.2007.03.003). *J Biomech*. 2008;41(10):2332-2333. doi:10.1016/j.jbiomech.2008.04.036.
 36. Selvik Gör. Roentgen stereophotogrammetry. *Acta Orthop*. 1989;60(s232):1-51.
doi:10.3109/17453678909154184.
 37. Bojan AJ, Bragdon C, Jönsson A, Ekholm C, Kärrholm J. Three-dimensional bone-implant movements in trochanteric hip fractures: Precision and accuracy of radiostereometric analysis in a phantom model. *J Orthop Res*. 2015;33(5):705-711. doi:10.1002/jor.22822.

38. Kärrholm J. Roentgen stereophotogrammetry. Review of orthopedic applications. *Acta Orthop Scand*. 1989;60(4):491-503. doi:10.3109/17453678909149328.
39. van Embden D, Stollenwerck G a. NL, Koster L a., Kaptein BL, Nelissen RGHH, Schipper IB. The stability of fixation of proximal femoral fractures: a radiostereometric analysis. *Bone Joint J*. 2015;97-B(3):391-397. doi:10.1302/0301-620X.97B3.35077.
40. Molt M, Toksvig-Larsen S. 2-Year Follow-Up Report on Micromotion of a Short Tibia Stem. *Acta Orthop*. 2015;86(5):594-598. doi:10.3109/17453674.2015.1033303.
41. Kaptein BL, Valstar ER, Stoel BC, Rozing PM, Reiber JHC. A new model-based RSA method validated using CAD models and models from reversed engineering. *J Biomech*. 2003;36(6):873-882. doi:10.1016/S0021-9290(03)00002-2.
42. Valstar ER, De Jong FW, Vrooman H a., Rozing PM, Reiber JHC. Model-based Roentgen stereophotogrammetry of orthopaedic implants. *J Biomech*. 2001;34(6):715-722. doi:10.1016/S0021-9290(01)00028-8.
43. Valstar ER, Gill R, Ryd L, Flivik G, Börlin N, Kärrholm J. Guidelines for standardization of radiostereometry (RSA) of implants. *Acta Orthop*. 2005;76(4):563-572. doi:10.1080/17453670510041574.
44. Valstar ER, Nelissen RGHH, Reiber JHC, Rozing PM. The use of Roentgen stereophotogrammetry to study micromotion of orthopaedic implants. *ISPRS J Photogramm Remote Sens*. 2002;56(5-6):376-389. <http://www.sciencedirect.com/science/article/pii/S0924271602000643>. Accessed January 10, 2016.
45. Derbyshire B, Prescott RJ, Porter ML. Notes on the use and interpretation of radiostereometric analysis. *Acta Orthop*. 2009;80(1):124-130. doi:10.1080/17453670902807474.
46. Stilling M. Polyethylene wear analysis: Experimental and clinical studies in total hip replacement. *Acta Orthop*. 2009;80(337). doi:10.3109/17453670903420819.
47. Martin DE, Greco NJ, Klatt BA, Wright VJ, Anderst WJ, Tashman S. Model-Based Tracking of the Hip: Implications for Novel Analyses of Hip Pathology. *J Arthroplasty*. 2011;26(1):88-97. doi:10.1016/j.arth.2009.12.004.

48. Soderkvist I, Wedin PA. Determining the movements of the skeleton using well-configured markers. *J Biomech.* 1993;26(12):1473-1477. doi:10.1016/0021-9290(93)90098-Y.
49. Selvik G. Roentgen stereophotogrammetric analysis. *Acta radiol.* 1990;31(2):113-126. doi:10.3109/02841859009177472.
50. Leardini A, Cappozzo A, Catani F, et al. Validation of a functional method for the estimation of hip joint centre location. *J Biomech.* 1999;32(1):99-103. doi:10.1016/S0021-9290(98)00148-1.
51. Stagni R, Leardini A, Cappozzo A, Grazia Benedetti M, Cappello A. Effects of hip joint centre mislocation on gait analysis results. *J Biomech.* 2000;33(11):1479-1487. doi:10.1016/S0021-9290(00)00093-2.
52. Kaptein BL, Valstar ER, Stoel BC. Clinical Validation of Model-based RSA for a Total Knee Prosthesis. 2007;(464):205-209. doi:10.1097/BLO.0b013e3181571aa5.
53. Stråling i sundhedsvidenskabelige forsøg. *Den Natl Vidensk komité.* 2011;2(December):2-4. <http://www.cvk.sum.dk/forskere/vejledning/modul/~media/Files/cvk/forskere/vejledning/Appendiks 2 strling 2012.ashx>.

Appendix

Dataset for kinematics article

The dataset consists of the donor hip id (cid), flexion-, internal rotation- (internal_rot) and abduction angles (the opposite of which is adduction), the stage referring to preoperative and postoperative, Tx, Ty and Tz are the translations of the femoral head center of rotation with respect to the pelvis along the x-, y- and z-axes.

cid	flexion	internal_rot	abduction	Tx	Ty	Tz	stage	recording	
KDA 1	79.596	12.653	6.609	1.332	1.807	-0.158	preop	0	dynamic
KDA 1	82.800	15.672	7.618	0.717	1.274	-0.582	postop	1	dynamic
KDB 2	81.602	12.456	-4.839	-0.467	3.052	0.956	preop	0	dynamic
KDB 2	78.414	20.621	-1.512	-1.052	1.886	-0.303	postop	1	dynamic
KDC 3	74.694	25.134	5.157	-0.063	1.095	-0.066	preop	0	dynamic
KDC 3	75.180	24.898	3.163	-0.687	1.688	1.472	postop	1	dynamic
KDE 4	85.023	15.605	-30.161	-1.181	2.422	-1.408	preop	0	dynamic
KDE 4	80.133	18.476	-26.340	-2.104	0.896	-1.721	postop	1	dynamic
KDF 5	86.589	36.561	-11.847	0.834	1.896	0.067	preop	0	dynamic
KDF 5	84.264	40.150	-3.705	2.329	1.934	-0.713	postop	1	dynamic
KDG 6	88.044	10.207	1.926	-4.366	0.735	-5.262	preop	0	dynamic
KDG 6	84.753	11.110	1.332	-5.111	0.958	-5.887	postop	1	dynamic
KDH 7	81.202	21.379	5.910	4.866	1.418	-3.697	preop	0	dynamic
KDH 7	80.195	22.608	0.795	4.650	2.411	-5.236	postop	1	dynamic

Results of the kinematic study

Summary of the migration data analysis with \pm LOA as the expected clinical precision. The total is calculated from the norm (3D-Pythagorean theorem) of translations and rotations.

Table 1 - Mean difference in rotations (°)

	Femur				Pelvis			
	Rx	Ry	Rz	Total	Rx	Ry	Rz	Total
Mean diff [†]	-0.001	-0.007	-0.01	0.400	0.008	-0.009	-0.009	0.334
SD _{diff} [‡]	0.267	0.361	0.188	0.276	0.296	0.201	0.243	0.275
\pm LOA [¶]	0.523	0.707	0.369	0.542	0.580	0.394	0.477	0.539
Minimum [§]	-0.738	-1.619	-0.620	0.016	-1.095	-0.629	-1.177	0.018
Maximum ^{**}	1.048	1.285	0.669	1.689	1.398	0.679	0.962	1.539

[†]Mean difference in rotations (degrees) between MBM and MM.

[‡]Standard deviation of the mean difference, random variation.

[¶]Limits of agreement 95% LOA, expected clinical precision.

[§]Minimum observed value.

^{**}Maximum observed value.

^{*}Statistically significantly different from zero, paired t-test.

Table 2 - Mean difference in translations (mm)

	Femur				Pelvis			
	Tx	Ty	Tz	Total	Tx	Ty	Tz	Total
Mean diff [†]	0.005	0.014 [*]	-0.002	0.213	-0.002	0.003	0.006	0.355
SD _{diff} [‡]	0.075	0.106	0.226	0.150	0.107	0.158	0.462	0.351
\pm LOA [¶]	0.146	0.208	0.443	0.293	0.209	0.310	0.905	0.688
Minimum [§]	-0.235	-0.312	-0.829	0.025	-0.381	-0.627	-1.499	0.002
Maximum ^{**}	0.290	0.414	0.669	0.868	0.436	0.648	1.933	1.958

[†]Mean difference in translations (mm) between MBM and MM.

[‡]Standard deviation of the mean difference, random variation.

[¶]Limits of agreement 95% LOA, expected clinical precision.

[§]Minimum observed value.

^{**}Maximum observed value.

^{*}Statistically significantly different from zero, paired t-test.